Pressure-induced structural phase transitions in the AMnF$_4$ series (A=Cs, Rb, K) studied by synchrotron x-ray powder diffraction: Correlation between hydrostatic and chemical pressure

M. C. Morón and F. Palacio

Instituto de Ciencia de Materiales de Aragón, Consejo Superior de Investigaciònes Cientificas, Universidad de Zaragoza,
E-50009 Zaragoza, Spain

S. M. Clark

Daresbury Laboratory, Warrington WA4 4AD, United Kingdom

The effect of applying hydrostatic pressure in the layered-perovskite AMnF$_4$ (A=Cs, Rb, K) series has been studied using energy-dispersive synchrotron x-ray powder diffraction at pressures between ambient and 20 GPa. At ambient pressure CsMnF$_4$ is tetragonal with space group $P4/n$, RbMnF$_4$ is orthorhombic with space group $Pmab$ and KMnF$_4$ is monoclinic with space group $P2_1/a$. CsMnF$_4$ was found to undergo a first-order structural phase transition, from tetragonal to orthorhombic symmetry at $P_{c_1}=1.4\pm0.2$ GPa. At pressures in excess of $P_{c_2}=6.3\pm1$ GPa, for the Cs derivative, and $P_{c_3}=4.5\pm1$ GPa, for the Rb derivative, the symmetry appears to be monoclinic. Moreover, the critical unit-cell volumes associated with P_{c_1}, P_{c_2}, and P_{c_3} are slightly higher than the ambient pressure unit-cell volumes of RbMnF$_4$ for P_{c_1} and KMnF$_4$ for P_{c_2} and P_{c_3}. Hydrostatic pressure has been found to have a similar effect on the crystal symmetry of the series as the decreasing of the radius of the alkaline ion from Cs to Rb and K. A correlation between hydrostatic and chemical pressure can therefore be established from the structural point of view for the AMnF$_4$ series. The tetragonal to orthorhombic transition of CsMnF$_4$ has been found to be inhibited when NaCl is used as an internal pressure calibrant. The partial substitution of Cs by Na in CsMnF$_4$ at P_{c_1} has been shown to be a likely explanation for this behavior. The anisotropic broadening of the Bragg peaks for pressures higher than P_{c_1} has been analyzed in terms of microstrain affecting the CsMnF$_4$ lattice due to Na incorporation. A substitutional reaction has been shown to be a competitive process, versus a structural phase transition, that enables the system to return to equilibrium after applying pressure on it. Finally, the equation of state associated with the different high-pressure phases has been calculated including compressibilities. [S0163-1829(96)06534-4]

I. INTRODUCTION

The AMnF$_4$ (A=Cs, Rb, K, Na) series of layered perovskites has been shown to exhibit a very interesting structural and magnetic behavior. An important characteristic of these Mn^{3+} compounds is the presence of strong Jahn-Teller distortions which severely affects their respective structures and magnetism.[1,2] Compounds of general formula AMnF$_4$ form layers of corner-sharing $[MF_2F_{4/2}]^-$ octahedra separated by the alkali ions in a structural arrangement of the TlAlF$_4$ type.[3] Throughout this work, we have adopted the convention of taking the c axis perpendicular to the layers. Thus, CsMnF$_4$ crystallizes in the tetragonal space group $P4/n$ with $a=7.9440(6)$ Å and $c=6.3376(9)$ Å,[4,5] RbMnF$_4$ has been refined in the orthorhombic space group $Pmab$ with $a=7.8051(8)$ Å, $b=7.7744(8)$ Å, and $c=6.0432(6)$ Å, and KMnF$_4$ crystallizes in the monoclinic space group $P2_1/a$ with $a=7.7062(2)$ Å, $b=7.6568(2)$ Å, $c=5.7889(1)$ Å, and $\beta=90.432(2)°$.[2] The pseudotetragonal Rb derivative has also been refined from neutron-diffraction data in the monoclinic space group $P2_1/a$ with $a=7.8119(4)$ Å, $b=7.7761(4)$ Å, $c=6.0469(3)$ Å, and $\beta=90.443(4)°$.[2] In addition, NaMnF$_4$ also crystallizes in the space group $P2_1/a$ with $a=5.760(2)$ Å, $b=4.892(1)$ Å, $c=5.755(2)$ Å, and $\beta=108.62(1)°$.[6] The atomic structures of CsMnF$_4$ and RbMnF$_4$ at ambient pressure are represented in Fig. 1. The atomic structure of KMnF$_4$ is very similar to that of RbMnF$_4$ with the octahedra in both compounds sharing the same tilting pattern. However, the magnitude of the tilt angles is larger for the K than for the Rb compound.

The magnetic behavior of these compounds also depends very strongly on the size of the alkali ion. Thus, neutron powder-diffraction experiments evidences that CsMnF$_4$ orders as a ferromagnet below 18.9 K, while the other members of the series exhibit antiferromagnetic ordering at lower temperatures. The magnetic moments are collinear for the Rb derivative but canted for the K and Na derivatives. The sign of the magnetic interaction and the value of the critical temperature are dramatically influenced by the value of the magnetic superexchange angle Mn-F-Mn, which strongly depends on the size of the alkali ion.[2]

As the size of the alkali ion decreases from Cs to K, the layers of $[MF_2F_{4/2}]^-$ octahedra get closer and electrostatic and steric forces rotate the octahedra within the layers causing a reduction of the crystal symmetry.[2] We could think of this process of bringing the layers of octahedra closer together as being due to the application of chemical pressure as the radius of the alkaline ion changes from Cs to Rb and K. So an analogous, although more continuous, method of reducing the interlayer spacing would be to apply an external
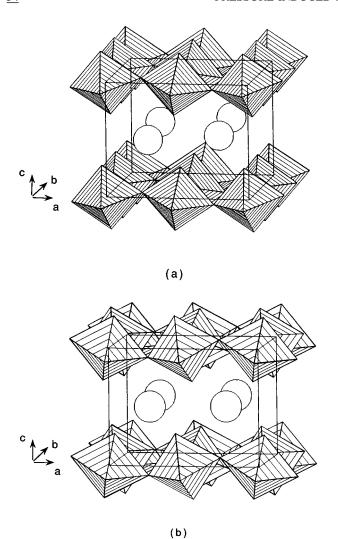
(a)

(b)

FIG. 1. Crystallographic unit cell of (a) CsMnF$_4$ and RbMnF$_4$ at ambient pressure and room temperature; octahedra stand for the [MnF$_2$F$_{4/2}$]$^-$ units while open circles for (a) the Cs and (b) the Rb atoms. The tilting scheme of the octahedra for KMnF$_4$ is that of RbMnF$_4$.

pressure to the member of the series with the largest unit-cell volume, i.e., CsMnF$_4$.

In this work we compare the effects of external and chemical pressure on the crystal symmetry of compounds AMnF$_4$. Some preliminary results together with some magnetic measurements made with the sample under hydrostatic pressure have already been published.[7] The paper is organized as follows. The experimental details are reported in Sec. II. The structural phase transitions which have been induced on the Cs and Rb derivatives by applying hydrostatic pressure are analyzed in Sec. III. In the course of our experiments, two different substances were used as internal pressure calibrants: Ag and NaCl. The strong differences found between these two sets of data are analyzed in Sec. IV. Finally, the equations of state and compressibilities of the different phases exhibited by CsMnF$_4$ and RbMnF$_4$ under pressure are also calculated in Sec. V, while concluding remarks are presented in Sec. VI.

II. EXPERIMENTAL DETAILS

Polycrystalline samples of CsMnF$_4$ and RbMnF$_4$ were prepared by controlled dehydration of CsMnF$_4\cdot$2H$_2$O and RbMnF$_4\cdot$H$_2$O at 120 °C. The hydrated compounds were synthesized following previously described methods.[8,9] Conventional x-ray powder-diffraction techniques were used to check that the compounds were of single phase and free of impurities.

Powder-diffraction spectra were collected at a series of different static pressures using the energy-dispersive powder diffraction (EDPD) facility at the Daresbury Laboratory Synchrotron Radiation Source (SRS).[10,11] The SRS operates at 2 GeV with typical stored electron beam currents in excess of 200 mA. The EDPD facility is situated 15 m from the tangent point and benefits from radiation emitted from two poles of a superconducting wiggler magnet of peak field 5 T. The facility receives useful x-ray flux in the range from 5 to 50 keV with a peak intensity of about 7×10^{11} photons/sec mm^2 in a 0.1% bandwidth at about 10 keV. The EDPD method uses a polychromatic beam of x-rays and a germanium solid-state detector set at a fixed scattering angle. The fixed geometry makes it straightforward to obtain good quality spectra, in a few minutes, from a sample contained in a high-pressure cell with little or no contamination from gasketting material. The EDPD method has the disadvantage that the momentum resolution is an order of magnitude lower than that obtained using monochromatic techniques. In this case we choose the EDPD method in order to survey the effect of pressure on these samples across a large pressure range with fine sampling. Diffraction patterns were collected for about 15 min at each pressure point. After each set of three or four diffraction patterns, the scattering angle was calibrated by using silicon as standard. The values obtained moved from $2\theta=5.760°$ to $2\theta=5.785°$.

A diamond-anvil cell was used to generate high pressures from ambient up to 20 GPa. Either Ag (Ref. 12) or NaCl (Ref. 13) were used as internal pressure standards. Inconel metal gaskets, with a 0.2 mm diameter sample hole, were used to contain the samples together with an ethanol-methanol-water mixture as the pressure transmitting medium.

Diffraction patterns were analyzed by using the GENIE data manipulation package.[14] Peak parameters were determined by fitting Gaussian profiles to each peak. Unit-cell parameters and unit-cell volumes were calculated by using the PDPL computer package.[15]

III. STRUCTURAL PHASE TRANSITIONS INDUCED BY PRESSURE

The influence of the external pressure on the structural properties of some series of compounds has been studied by different authors.[16–20] In our case, the experimental data were analyzed in order to study the evolution of the crystal symmetry of CsMnF$_4$ as a function of pressure and to compare these results with the crystal symmetry of the other members of the AMnF$_4$ layered-perovskite family. Most of the members of this series exhibit a strong pseudotetragonal symmetry.[2] Therefore, special care was taken in the analysis
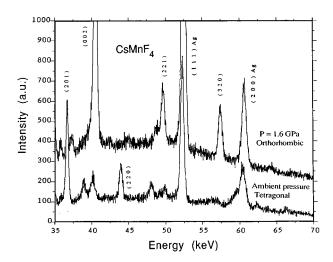
FIG. 2. Synchrotron x-ray powder-diffraction data taken on CsMnF$_4$ at ambient pressure and at 1.6 GPa. Some relevant reflections are shown. Below 36 keV only fluorescence peaks appear.

FIG. 4. Synchrotron x-ray-diffraction patterns collected on RbMnF$_4$ (orthorhombic) and KMnF$_4$ (monoclinic) at ambient pressure. The unit cell of both compounds is pseudosymmetric.

of the data from the crystallographic point of view. To determine the crystal symmetry of the high-pressure phases, the very small difference exhibited by the a and b unit-cell parameters was taken into account.

A. Tetragonal to orthorhombic

The diffraction pattern collected at ambient pressure on CsMnF$_4$ (see Fig. 2), can be indexed in the tegragonal space group $P4/n$, in good agreement with the reported crystal structure of this compound. For pressures higher than 1.5 GPa the diffraction patterns can no longer be satisfactorily indexed using this space group. They exhibited reflections such as $hk0$ with $h+k \neq 2n$ (see Fig. 2) which are forbidden in the space group $P4/n$. At pressures higher than 1.5 GPa the a and b unit-cell parameters refine to values that are different within the experimental error (see Fig. 3). Splitting of the Bragg peaks associated with the difference of a and b
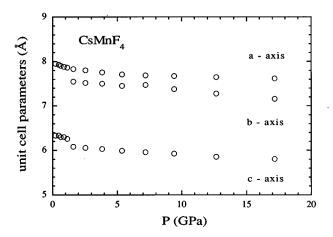

FIG. 3. Dependence of the unit-cell parameters of CsMnF$_4$ with the pressure along the tetragonal, orthorhombic, and monoclinic phases. The critical pressures are, respectively, $P_{c_1} = 1.4 \pm 0.2$ GPa and $P_{c_2} = 6.3 \pm 1$ GPa. The error bars are smaller than the size of the circles.
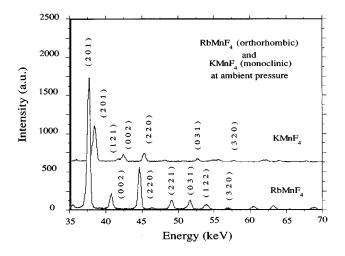
parameters were looked for in the diffraction patterns collected at pressures higher than 1.5 GPa. Unfortunately, the strong pseudotetragonal symmetry exhibited by this family of layered perovskites prevents the observation of splitting of the Bragg peaks in the orthorhombic phase as it is shown in the diffraction pattern of orthorhombic RbMnF$_4$ taken at ambient pressure by using the EDPD technique (see Fig. 4). No splitting is detected when the peaks are analyzed by fitting Gaussian profiles to each peak. Even by using standard monochromatic techniques, which have momentum resolution higher than the EDPD method, the splitting of the Bragg peaks is not observed for orthorhombic RbMnF$_4$ precisely due to the strong pseudotetragonal character of the compound.[2] The reflections $hk0$ with $h+k \neq 2n$ exhibited by orthorhombic CsMnF$_4$ are permitted for the orthorhombic space group $Pmab$. In fact, the diffraction patterns in this phase can be indexed in the space group $Pmab$. Within the limitations of the x-ray-diffraction technique we are using here, RbMnF$_4$ can be well described at ambient pressure in this space group.

The dependence of the unit-cell volume of CsMnF$_4$ with the pressure shows a clear discontinuity associated with the structural phase transition from tetragonal to orthorhombic symmetry (see Fig. 5). From these data a critical pressure of $P_{c_1} = 1.4 \pm 0.2$ GPa and a volume decrease of 6.5%, from 387 to 360 Å^3, can be estimated. The discontinuity of the unit-cell volume at P_{c_1} suggests a first-order character of the tetragonal to orthorhombic phase transition. Then, a group-subgroup relationship should not be expected in the space groups of the tetragonal and orthorhombic CsMnF$_4$ phases. This fact does not disagree with the possibility of assigning $Pmab$ as the space group of orthorhombic CsMnF$_4$ since $Pmab$ is not a subgroup of $P4/n$. The indexing of the pattern corresponding to take off the pressure by mechanical methods from 18 GPa evidences an orthorhombic symmetry. In this case, the internal pressure calibrant (Ag) shows that the sample was still experiencing a residual pressure of 0.9 ± 0.3 GPa which indicates that the pressure was not completely released. Although this value is too close to P_{c_1} to establish, within experimental error, that CsMnF$_4$ is actually at P
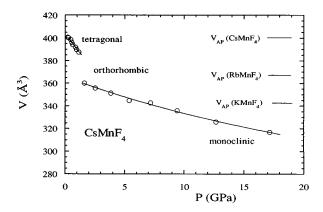
FIG. 5. Evolution with pressure of the unit-cell volume of $CsMnF_4$ as determined from room-temperature synchrotron x-ray powder-diffraction data. A structural phase transition takes place at 1.4 ± 0.2 GPa and another at 6.3 ± 1 GPa. The data have been fitted to a Birch equation of state (see text for details). The volume of the Cs, Rb, and K derivatives at ambient pressure are also depicted.

$< P_{c_1}$ it might be indicative of the hysteretic character of the tetragonal to orthorhombic structural phase transition. Room-temperature high-pressure Raman experiments have been carried out on single crystals of the layered-perovskite related compound $KFeF_4$. Interestingly enough, the authors conclude that $KFeF_4$ undergoes a discontinuous (first-order) phase transition at 1.2 GPa, with the high-pressure phase having $Pmab$ symmetry.[21]

The abrupt change in the unit-cell volume at $P_{c_1} = 1.4$ GPa is due to the discontinuity exhibited by the b and c parameters at that point (see Fig. 3). As already mentioned, the c axis is perpendicular to the layers of octahedra. As expected, these data indicate that as pressure is applied on this sandwich-type compound the distance between adjacent layers decreases. The epitaxy between the A cation and the layers of octahedra produces a stress in the structure, which is partially relieved by tilting the octahedra. Such stress, and therefore the magnitude of the tilt angles, is inversely proportional to the radius of the alkaline ion.[2] It is interesting to point out the different behavior exhibited by the two intra-layer unit-cell parameters at P_{c_1}. A continuity is observed along a but a discontinuity along b. The tilting scheme around the crystallographic axes is depicted in Fig. 6 for the Cs (tetragonal $P4/n$) and Rb (orthorhombic $Pmab$) derivatives at ambient pressure. Interestingly enough, the tilting of the octahedra around the b axis is not the same for the tetragonal than for the orthorhombic space groups. However, such a tilting scheme is the same along the a axis for both symmetries.

Pressure-induced phase transitions have been classified into four categories by Gupta and Chidambaram.[22] This classification is based on the structural and symmetry relationship between the initial and the final phases and it is important in order to understand the mechanism of pressure-induced phase transitions. These four categories are (i) Isosymmetric transitions, when the parent and product phases have the same space-group symmetry although the crystal structure can be different, (ii) Group-subgroup transitions,
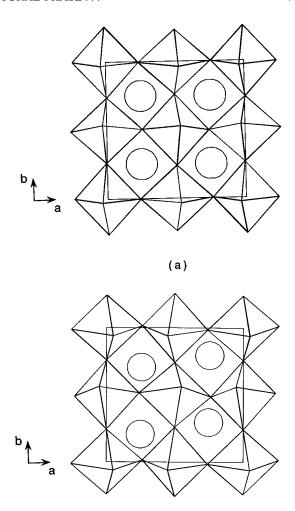

(a)

(b)

FIG. 6. [001] view of the ambient pressure unit cell of (a) $CsMnF_4$ (tetragonal $P4/n$) and (b) $RbMnF_4$ (orthorhombic $Pmab$), showing the tilting scheme of the octahedra around the crystallographic axes. The tilting scheme of $KMnF_4$ (monoclinic $P2_1/a$) is that of the Rb derivative.

when the initial and final phases have a group-subgroup (or supergroup) relationship, (iii) Intersection group transitions, when the space group of the final phase is not a subgroup (or supergroup) of the space group of the initial phase but both phases have a common subgroup (intersection group), (iv) Order-disorder transitions, that is crystalline to amorphous phase transitions. If $Pmab$ were effectively the space group of the high-pressure phase then the tetragonal-orthorhombic phase transition would belong to the category (iii) of Gupta and Chidambaram since $Pmab$ is not a subgroup of $P4/n$. When analyzing the group-subgroup relationship concerning these two space groups, $P2/c$ is found to be a common subgroup (intersection group). Following Gupta *et al.*, the pressure-induced structural phase transition that $CsMnF_4$ shows at 1.4 GPa could proceed via an intermediate phase of $P2/c$ symmetry. Such a $P2/c$ phase has not been detected during the process of analyzing the diffraction patterns. In fact, an intermediate structure in an intersection group transition is generally thermodynamically unstable and may not be observed during the transition.
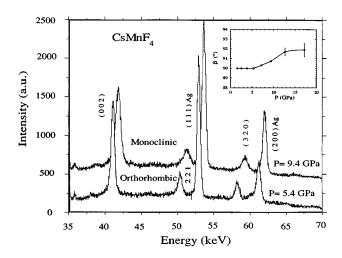
FIG. 7. Synchrotron x-ray powder-diffraction data taken on CsMnF$_4$ at 5.4 and 9.4 GPa. The β angle departs from 90° as the crystal symmetry change from orthorhombic to monoclinic (see insert). The error bars not visible are smaller than the size of the circles.

B. Orthorhombic to monoclinic

At pressures higher than 6 GPa the β angle refines to values that within the experimental error are different from 90° (see inset of Fig. 7) indicative of a further reduction, now from orthorhombic to monoclinic, of the crystal symmetry. Two diffraction patterns corresponding to 5.4 GPa, orthorhombic, and to 9.4 GPa, monoclinic, are shown in Fig. 7. The change in the evolution of the β angle with pressure is quite small although noticeable (see inset). The a, b, and c unit-cell parameters of monoclinic CsMnF$_4$ are depicted in Fig. 3. As in the case of the tetragonal to orthorhombic phase transition the strong pseudosymmetry exhibited by these layered perovskites prevents the observation of the splitting of the Bragg peaks associated with the departure of the β angle from 90° as it is shown in the diffraction pattern of monoclinic KMnF$_4$ taken at ambient pressure by using the EDPD technique (see Fig. 4). No splitting is detected when the peaks are analyzed by fitting Gaussian profiles to each peak. Even by using standard monochromatic techniques, which have momentum resolution higher than the EDPD method, such a splitting of the Bragg peaks is not observed for KMnF$_4$ due to the pseudosymmetry of the unit cell.[2]

The space group of ambient pressure KMnF$_4$, $P2_1/a$, belongs to the monoclinic symmetry. The diffraction patterns of CsMnF$_4$ for pressures higher than 6 GPa can be indexed in such a space group. Concerning reflection conditions, the only difference between the space groups $Pmab$ and $P2_1/a$ is that the $hk0$ reflections with k odd are forbidden for $Pmab$ but permitted for $P2_1/a$ symmetry. The intensity of these reflections has been simulated for CsMnF$_4$ considering a $P2_1/a$ symmetry and a structural model corresponding to that of KMnF$_4$. Within the energy range considered these reflections are expected to be very weak and therefore hardly detectable using the high-pressure EDPD technique. This would explain why this set of reflections have not been found in the diffraction patterns of CsMnF$_4$ for $P>6$ GPa and in KMnF$_4$ at ambient pressure (see Fig. 4 and Ref. 2). Further experiments with higher range and resolution in mo-
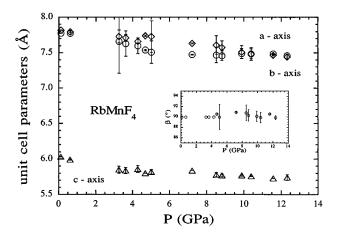

FIG. 8. Evolution of the unit-cell parameters of RbMnF$_4$ with the pressure for both orthorhombic and monoclinic phases. The corresponding critical pressure is $P_{c_3}=4.5\pm1$ GPa.

mentum would be desired in order to determine without ambiguity the space group of monoclinic CsMnF$_4$.

The unit-cell volume of monoclinic CsMnF$_4$ as a function of the applied pressure is depicted in Fig. 5. A critical pressure of $P_{c_2}=6.3\pm1$ GPa and an associated critical volume of $V_{c_2}=344\pm5$ Å^3 can be estimated for the orthorhombic to monoclinic structural phase transition. No detectable discontinuity in the evolution of the unit-cell volume with pressure is observed. The fact that there is a continuous transformation path evidences the close structural relationship of the orthorhombic and monoclinic high-pressure phases. Such a close structural relationship is also exhibited by the crystal structure of the Rb, space group $Pmab$, and the K space group $P2_1/a$, derivatives.[2] If $P2_1/a$ and $Pmab$ were effectively the space groups of, respectively, monoclinic and orthorhombic CsMnF$_4$ then the phase transition we considered here would clearly belong to the group-subgroup category of Gupta $et\ al.$ since $P2_1/a$ is a subgroup of $Pmab$.

The behavior of RbMnF$_4$ with pressure has been also studied for comparison with that of CsMnF$_4$. The EDPD pattern obtained for RbMnF$_4$ at ambient pressure indicates that the crystal symmetry is orthorhombic with space group $Pmab$, in good agreement with previous determinations. Following a procedure completely similar to that described in Sec. III B for CsMnF$_4$ we have found that RbMnF$_4$ exhibits a transition from a orthorhombic to a monoclinic symmetry at $P_{c_3}=4.5\pm1$ GPa. The dependence of the unit-cell parameters and unit-cell volume of RbMnF$_4$ with pressure is shown in Fig. 8. As in the case of CsMnF$_4$, the change in symmetry at P_{c_3} is quite subtle but noticeable in the evolution of the β angle with pressure. However, the occurrence of such a transition is clearer in the case of the Cs derivative than in RbMnF$_4$ since the departure from $\beta=90°$ is more important in the first compound than in the second (e.g., compare Figs. 7 and 8). On the other hand, orthorhombic and monoclinic CsMnF$_4$ exhibits higher c unit-cell values than RbMnF$_4$ in excellent agreement with the higher radius of the Cs versus the Rb ions. The dependence of the unit-cell volume of RbMnF$_4$ with pressure is depicted in Fig. 9. As in the case of CsMnF$_4$ no discontinuity is observed at the occurrence of the orthorhombic to monoclinic structural phase
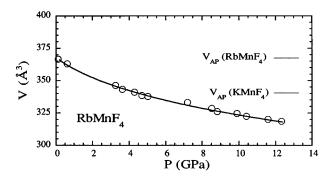
FIG. 9. Dependence of the unit-cell volume of $RbMnF_4$ with pressure at ambient temperature. A structural phase transition occurs at 4.5 GPa from an orthorhombic to a monoclinic symmetry. The data have been fitted to a Birch equation of state (see text for details). The volume of the Rb and K derivatives at ambient pressure are also depicted.

transition. A critical unit-cell volume associated with P_{c_3} can be estimated for $RbMnF_4$ as $V_{c_3} = 340 \pm 5$ $Å^3$.

C. Pressure correlations

The critical pressure which is necessary to apply to $CsMnF_4/RbMnF_4$ to change from tetragonal/orthorhombic to orthorhombic/monoclinic is $P_{c_1} = 1.4 \pm 0.2$ $GPa/P_{c_3} = 4.5 \pm 1$ GPa. The total pressure required for $CsMnF_4$ to change from tetragonal to monoclinic is $P_{c_2} = 6.3 \pm 1$ GPa. However, 1.4 GPa have already been used to transform the symmetry from tetragonal to orthorhombic. Therefore the actual pressure required for $CsMnF_4$ to change from orthorhombic to monoclinic turns out to be $P_{c_2} - P_{c_1} = 6.3 - 1.4 = 4.9 \pm 1$ GPa. It can be worth observing that this value matches, within the experimental error, $P_{c_3} = 4.5 \pm 1$ GPa which is the pressure required for $RbMnF_4$ to change from orthorhombic to monoclinic. The critical pressure associated to the orthorhombic to monoclinic phase transition does not seem to depend, within the experimental error, on the nature of the alkaline ion. Remark that the correctness of this last statement relies on the assumption of a tetragonal to orthorhombic phase transition near 0 GPa for $RbMnF_4$.

The critical volume associated with the orthorhombic to monoclinic transition of $CsMnF_4$, $V_{c_2} = 344 \pm 5$ $Å^3$, and $RbMnF_4$, $V_{c_3} = 340 \pm 5$ $Å^3$, coincides within experimental uncertainties. This suggests that the critical volume of the orthorhombic to monoclinic phase transition is independent of the nature of the alkaline ion A. Then, a critical volume of 342 ± 5 associated with the orthorhombic to monoclinic phase transition on the $AMnF_4$ series has been calculated as the mean value between V_{c_2} and V_{c_3}.

At this point it is important to remember that the data shown in Figs. 5 and 9, crystal symmetry of the $AMnF_4$ series as a function of both pressure and unit-cell volume, have been obtained by applying hydrostatic pressure. Chemical pressure is applied along the $AMnF_4$ series, by reducing the radius of the alkaline ion from Cs to K. The result of this chemical pressure acting on $CsMnF_4$ would be represented, in a first step, by $RbMnF_4$. This compound has orthorhombic symmetry and unit-cell volume of 367 $Å^3$. Hydrostatic pres-

sure applied on $CsMnF_4$ suggests that for unit-cell volumes smaller than 387–360 $Å^3$ the crystal symmetry can no longer be tetragonal but orthorhombic (387 and 360 $Å^3$ correspond to the limits on volume of the first-order tetragonal to orthorhombic transition). Both hydrostatic and chemical pressure effects are in agreement. The next representative compound that reflects the effects of an increase of chemical pressure is $KMnF_4$ that possess a unit-cell volume of 341 $Å^3$ and a monoclinic symmetry. Hydrostatic pressure indicates that for unit-cell volumes smaller than 342 $Å^3$ the crystal symmetry can no longer be orthorhombic but monoclinic. Once again hydrostatic and chemical pressure effects are in agreement. As a result, hydrostatic pressure is found to have a similar effect on the crystal symmetry of these layered perovskites than chemical pressure as the radius of the alkaline ion decreases from Cs to Rb and K. A correlation between hydrostatic and chemical pressure can then be stated.

IV. INHIBITION OF THE TETRAGONAL TO ORTHORHOMBIC STRUCTURAL PHASE TRANSITION

In this section the differences observed on the evolution of the crystal symmetry of $CsMnF_4$ when using silver or sodium chloride as internal pressure calibrant are reported. In the low-pressure range NaCl is considered to be a more sensitive pressure calibrant than Ag since it has a larger compressibility. The diffraction patterns showing the occurrence of the two structural phase transitions presented in the previous section were collected by using silver as pressure calibrant. Further synchrotron EDPD experiments were performed on $CsMnF_4$ up to 2.5 GPa following the same experimental conditions already specified but using sodium chloride instead of silver. When sodium chloride is used as internal pressure calibrant, the diffraction patterns can be indexed in the tetragonal $P4/n$ symmetry within the whole pressure range. The fact that $CsMnF_4$ keeps the tetragonal symmetry from ambient up to 2.5 GPa implies that the tetragonal to orthorhombic structural phase transition no longer occurs (see Fig. 10). The pressure dependence of the lattice parameters and unit-cell volume of $CsMnF_4$ shows no discontinuity for the NaCl data set but just a subtle inflection point at 1.3 ± 0.2 GPa (see Fig. 10).

The existence of truly hydrostatic conditions was checked. The pressure transmitting medium used in both Ag and NaCl sets of experiments was 16:4:1 methanol-ethanol-water mixture which is hydrostatic up to 15 GPa and quasi-hydrostatic up to 20 GPa. If hydrostatic conditions do not hold, then the sample in the diamond-anvil cell will be affected by an anisotropic stress component. In cubic lattices, the most obvious consequence of such an stress is an hkl dependence of the lattice parameter.[23,24] We have calculated the unit-cell parameter of silver and sodium chloride from different hkl reflections at a variety of pressures. For each pressure, the differences between the calculated unit-cell parameters were found to be smaller than 1%. Therefore, we can conclude that the experiments here reported were performed under hydrostatic conditions. Consequently, the presence of anisotropic stress components acting on $CsMnF_4$ should be ruled out as the origin of the inhibition of the tetragonal to orthorhombic structural phase transition.
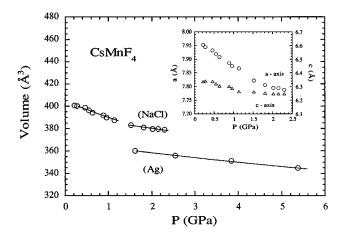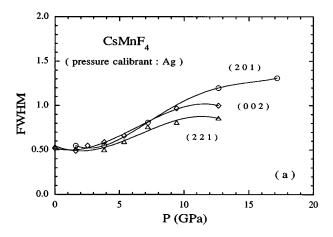
FIG. 10. Dependence of the unit-cell volume and lattice parameters of CsMnF$_4$ when using sodium chloride as internal pressure calibrant. The tetragonal to orthorhombic structural phase transition, occurring at $P_{c_1} = 1.4$ GPa when using silver as internal pressure calibrant, is inhibited. The data have been fitted to a Birch equation of state (see text for details).

The dependence with pressure of the full width at half maximum (fwhm) of the Bragg peaks has been also analyzed. For the case of data collected using Ag as an internal standard the fwhm remains constant, at a value of 0.5 °, up to 4 GPa for all the CsMnF$_4$ hkl reflections [see Fig. 11(a)]. However, the fwhm departs from such a constant value at much lower pressures in the case of the NaCl data collected with NaCl as an internal standard [Fig. 11(b)]. For the NaCl data set, the evolution of the fwhm with pressure shows an inflection point at 1.3 ± 0.1 GPa. This broadening is anisotropic in character since not all the reflections are affected. A wider energy range would be necessary to obtain an accurate symmetry law governing such a nonisotropic broadening. It can be concluded that when using NaCl as pressure calibrant, CsMnF$_4$ suffers from microanisotropic strain for pressures higher than 1.3 ± 0.1 GPa. It is interesting to observe that this value nicely fits with the critical pressure obtained for the tetragonal to orthorhombic structural phase transition which takes place at $P_{c_1} = 1.4 \pm 0.2$ GPa.

A likely explanation of these experimental features is the partial substitution of Cs by Na in CsMnF$_4$ in the vicinity of the (low pressure) structural phase transition. In fact, the reactivity of many solids has been found to be high in the neighborhood of phase transitions. This was suggested by Hedwall and is often referred to as the *Hedwall effect*.[25,26] Additional facts are in good agreement with the proposed pressure-induced substitutional reaction: (i) the microanisotropic strain described above would be the result of the stress created in the CsMnF$_4$ lattice by partially substituting Cs by Na, (ii) the broadening of the Bragg peaks associated with the microanisotropic strain is observed just in the proximities of P_{c_1}, (iii) since the unit-cell volume of NaMnF$_4$ is smaller than that of CsMnF$_4$ this substitution would stabilize the Na containing phase since this phase is a high-pressure one, (iv) a change in compressibility, expected for the Na containing phase when compared with tetragonal non-Na-containing CsMnF$_4$, is observed experimentally at a pressure P_{c_1} (see Fig. 10 and Table I), (v) such a pressure-induced substitu-
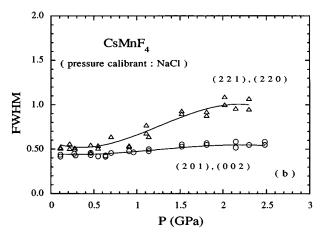

FIG. 11. Dependence with pressure of the full with at half maximum (FWHM) for CsMnF$_4$ Bragg peaks when using (a) silver or (b) sodium chloride as internal pressure calibrant.

tional reaction would be a simple consequence of the Le Chatelier–Braun principle, which allows a subtle interpretation of the way in which a system returns to the equilibrium state: "while a system tries to reduce a external perturbation, other processes may be also induced which can lead to a competitive ground state." If the extent of a reaction (or degree of progress of a reaction) is represented by the variable ξ, then the evolution of ξ with pressure can be written in terms of the affinity A, the Gibbs function G, and the variation of the reaction volume $\Delta_r V$:

$$(\delta\xi/\delta P)_{T,A} = -(\delta A/\delta P)_{T,\xi}/(\delta A/\delta\xi)_{T,P} = -\Delta_r V/G'', \quad (1)$$

where $A = -(\delta G/\delta\xi)_{T,P}$, and $G'' = (\delta^2 G/\delta\xi^2)_{T,P}$. The effect of P on ξ will depend only on the sign of $\Delta_r V$ since G'' is positive.[27] These expressions together with the fact that the unit-cell volume of NaMnF$_4$ is smaller than that of CsMnF$_4$ suggest that the pressure will favor the proposed substitutional reaction.

V. EQUATION OF STATE AND COMPRESSIBILITIES

A knowledge of compressibilities is essential for investigating the behavior of a given system under pressure. To determine the bulk modulus, which is the inverse of the com-

TABLE I. Zero-pressure isothermal bulk moduli B_0, compressibilities K_0, and unit-cell volumes V_0, for the different phases that $CsMnF_4$ and $RbMnF_4$ exhibit as a function of pressure.

Compound	Symmetry	B_0 (GPa)	$K_0 \times 10^3$ (GPa^{-1})	V_0 (Å^3)
$CsMnF_4$	Tetragonal	25±1	40.0±1.6	404.8±0.5
$CsMnF_4$ (+Na)[a]	Tetragonal	68±8	16.7±2.2	392.0±2.0
$CsMnF_4$	Orthorhombic	73±3	13.7±0.6	367.8±0.7
$CsMnF_4$	Monoclinic	81±5	12.3±0.8	369.0±2.0
$RbMnF_4$	Orthorhombic	49±2	20.4±0.8	367.5±0.6
$RbMnF_4$	Monoclinic	88±5	11.4±0.7	356.0±2.0

[a]Phase which has been obtained when using NaCl as internal pressure calibrant (see text for details).

pressibility, we have analyzed our data using the Birch equation of state[28] which expresses pressure as a series in the strain f:

$$P = 3B_0 f(1+2f)^{5/2}[1+af+bf^2+\cdots], \qquad (2)$$

where a and b are parameters related to the first- and second-order pressure derivatives of the bulk modulus, B_0 stands for the isothermal bulk modulus at zero pressure, and f is equal to $[(V_0/V)^{2/3}-1]/2$ V_0 and V being, respectively, the volumes at zero and at P pressures. The Birch equation of state provides an excellent description of the compression of most solids.[17,29–32] As many terms are introduced as are needed to fit satisfactorily the data. Inclusion of the bf^2 term is usually unnecessary. The relation of a with B_0', the first pressure derivative of the bulk modulus, is given by the expression $B_0'=(2a/3)+4$. Compression data for a wide variety of substances have been properly described by using the value $B_0'=4$, which corresponds to $a=0$.[30,32] From the knowledge of B_0, B_0', B_0'', etc., it is possible to calculate, for a given substance, the bulk modulus $B=-V/(\delta P/\delta V)$ and the compressibility $K=-(1/V)(\delta V/\delta P)$. Thus, B can be obtained by differentiation of (2) with respect to volume. In the limit of small compressions, that is for small P/B_0 ratio, B can be approached by a series expansion in powers of P:[28]

$$B = B_0 + B_0'P + B_0''P^2 + \cdots, \qquad (3)$$

where the first two terms usually suffice to represent low-pressure measurements.

Table I shows the B_0, V_0, and K_0 values calculated for the different phases of $CsMnF_4$ and $RbMnF_4$. They were calculated with $B_0'=4$ since the data were properly fitted terminating the series at the $a=0$ level in Eq. (2). Extrapolation of the fitted curves beyond the stability range of a given phase has limited meaning. The uncertainties of the extrapolated fit parameters reflect only statistical errors. Table I indicates that K_0 is higher for the tetragonal than for the orthorhombic and monoclinic $CsMnF_4$ phases. In a similar way, K_0 is higher for orthorhombic than for monoclinic $RbMnF_4$. These results are in good agreement with the general rule that the bulk modulus of high-pressure phases should be higher than those of the low-pressure phases. When NaCl is used as pressure calibrant, the partial substitution of Cs by Na gives rise to a sodium containing phase which exhibits a similar compressibility to that corresponding to $CsMnF_4$ after the occur-

rence of the low-pressure phase transition. Moreover, orthorhombic $RbMnF_4$ is more compressible than orthorhombic $CsMnF_4$, as expected from the smaller ionic radius of the Rb ion as compared to the Cs ion. A correlation has been experimentally found between the bulk modulus B_0 and the critical pressure P_c along the $AMnF_4$ series. Figure 12 suggests that P_c increases with B_0, as similarly found along the family of semiconductors I-III-VI$_2$ (I=Ag, Cu; III=Ga, In; VI=S, Se, Te).[33]

VI. CONCLUDING REMARKS

Firstly, our results show a correlation between hydrostatic and chemical pressure within the layered-perovskite $AMnF_4$ series (A=Cs, Rb, K). The effect of applying hydrostatic pressure on the $AMnF_4$ family affects the crystal symmetry of these series in a similar way that the application of chemical pressure does. Chemical pressure is applied along the $AMnF_4$ series by decreasing the radius of the alkaline ion from Cs to Rb and to K. The crystal symmetry of $CsMnF_4$ changes from tetragonal to orthorhombic at $P_{c_1}=1.4\pm0.2$ GPa. $RbMnF_4$ is orthorhombic, space group $Pmab$, at ambient pressure. If pressure continues being increased, a transition to a monoclinic symmetry appears to occur at $P_{c_2}=6.3\pm1$ GPa. $KMnF_4$ is monoclinic, space group $P2_1/a$, at ambient pressure. $RbMnF_4$ exhibits similar changes in the
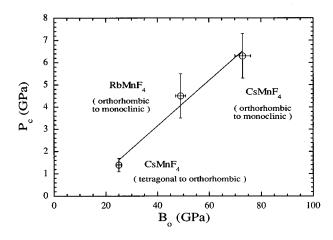

FIG. 12. Correlation between P_c, critical pressure, and B_0, isothermal bulk modulus at zero pressure, within the $AMnF_4$ series.

crystal symmetry from orthorhombic to monoclinic, with a smaller critical pressure $P_{c_3} = 4.5 \pm 1$ GPa. The comparison between the dependence of the unit-cell volume of the AMnF$_4$ compounds with hydrostatic and chemical pressures supports from the structural point of view the correlation between these two kind of pressures along this family of layered perovskites.

The sharpness of the tetragonal to orthorhombic phase transition suggests more significant structural changes associated with this first-order transition than those expected for the continuous path associated with the orthorhombic to monoclinic transition. This is in good agreement with the reported crystal structure at ambient pressure of the members of the AMnF$_4$ series. Although monoclinic $P2_1/a$ (space group of KMnF$_4$ at ambient pressure) is a subgroup of orthorhombic $Pmab$ (space group of RbMnF$_4$ at ambient pressure), this space group is not a subgroup of tetragonal $P4/n$ (space group of CsMnF$_4$ at ambient pressure). Further experiments with higher range and resolution in momentum would be desired to determine without ambiguity the space groups of the high-pressure phases.

The partial substitution of Cs by Na in CsMnF$_4$ at P_{c_1} has been shown to be a likely explanation for the absence of the tetragonal to orthorhombic phase transition detected when using NaCl as internal pressure calibrant. The smaller volume of NaMnF$_4$ versus that of CsMnF$_4$ would suggest that an increase of pressure on CsMnF$_4$ will favor the proposed substitutional reaction. The anisotropic broadening of the Bragg peaks observed for pressures higher than P_{c_1}, suggesting the presence of microstrains in the CsMnF$_4$ lattice, also supports the partial substitution of Cs by Na at P_{c_1}. There-fore, a substitutional reaction has been shown to be a competitive process, versus a structural phase transition, that enables the system to return to equilibrium after applying pressure on it.

If the tetragonal to orthorhombic phase transition is suppressed by a partial substitution of Cs by Na in CsMnF$_4$, then the compressibility of that Na-containing new phase is similar to that of orthorhombic CsMnF$_4$. On the other hand, orthorhombic RbMnF$_4$ is more compressible than orthorhombic CsMnF$_4$, as expected from the difference in the ionic radius of both ions. A correlation between the critical pressure and the zero-pressure isothermal bulk modulus has been also experimentally observed along the AMnF$_4$ series. This correlation suggests that the higher the value of B_0 for the low-pressure phase, the higher is the corresponding critical pressure.

Finally, it would be also very interesting to investigate if the parallelism between hydrostatic and chemical pressure also holds for the magnetic behavior of this interesting family of layered perovskites. If this is true, a transition from a ferromagnetic to an antiferromagnetic state should be induced on CsMnF$_4$ by applying pressure.

[1] F. Palacio and M. C. Morón, in *Research Frontiers in Magnetochemistry*, edited by C. J. O'Connor (World Scientific, Singapore, 1993), p. 227.

[2] M. C. Morón, F. Palacio, and J. Rodríguez-Carvajal, J. Phys. Condens. Matter **5**, 4909 (1993).

[3] K. S. Aleksandrov, B. V. Beznosikov, and S. V. Misyul, Ferroelectrics **73**, 201 (1987).

[4] W. Massaand M. Steiner, J. Solid State Chem. **32**, 137 (1980).

[5] J. Rodríguez-Carvajal, Physica B **192**, 55 (1993).

[6] M. Molinier, W. Massa, S. Khairoun, A. Tressaud, and J. L. Soubeyroux, Z. Naturforsch. **46**, 1669 (1991).

[7] M. C. Morón, F. Palacio, S. M. Clark, and A. Paduan-Filho, Phys. Rev. B **51**, 8660 (1995).

[8] V. Kaucic and P. Bukovec, J. Chem. Soc. Dalton Trans. **10**, 1512-15 (1979).

[9] F. Palacio, M. Andrés, C. Esteban-Calderón, and M. Martínez-Ripoll, J. Solid State Chem. **76**, 33 (1988).

[10] S. M. Clark, Rev. Sci. Instrum. Methods Phys. Res. Sect. A **276**, 381 (1989).

[11] S. M. Clark, Rev. Sci. Instrum. **63**, 1010 (1992).

[12] W. J. Carter, Nat. Bur. Stand. Spec. Publ. **326**, 147 (1971).

[13] D. L. Decker, J. Appl. Phys. **42**, 3239 (1971).

[14] W. I. F. David, M. W. Johnson, K. J. Knowles, C. M. Moreton-Smith, G. D. Crosbie, E. P. Campbell, S. P. Graham, and J. S. Lyall (unpublished).

[15] A. D. Murray, J. K. Cockcroft, and A. N. Fitch, *Powder Diffraction Program Library* (University College, London, 1990).

[16] J. M. Léger, J. Haines, and A. Atouf, J. Appl. Crystallogr. **28**, 416 (1995).

[17] S. Hull and D. A. Keen, Phys. Rev. B **50**, 5868 (1994).

[18] Y. Fujii, K. Hase, Y. Ohishi, H. Fujihisa, N. Hamaya, K. Takemura, O. Shimomura, T. Kikegawa, Y. Amemiya, and T. Matsushita, Phys. Rev. Lett. **63**, 536 (1989).

[19] K. Gesi, Ferroelectrics **66**, 269 (1986).

[20] Y. Yamada, M. Mori, and Y. Noda, J. Phys. Soc. Jpn. **32**, 1565 (1972).

[21] Q. Wang, A. Bulou, A. Désert, and J. Nouet, J. Phys. Condens. Matter **7**, 825 (1995).

[22] S. C. Gupta and R. Chidambaram, High Pressure Res. **12**, 51 (1994).

[23] A. K. Singh and G. C. Kennedy, J. Appl. Phys. **45**, 4686 (1974).

[24] A. K. Singh and C. Balasingh, J. Appl. Phys. **48**, 5338 (1977).

[25] J. A. Hedvall, *Reactionsfaehigkeit Fester Stoffe* (Verlag Johann Ambrosium Barth, Leipzig, 1938).

[26] C. N. R. Rao and K. J. Rao, *Phase Transitions in Solids: An Approach to the Study of Chemistry and Physics of Solids* (McGraw-Hill, New York, 1978).

[27] J. Güemez, S. Velasco, and M. A. Matías, J. Chem. Educ. **72**, 199 (1995).

[28] F. Birch, J. Geophys. Res. **83**, 1257 (1978).

[29] J. M. Besson, G. Weill, G. Hamel, R. J. Nelmes, J. S. Loveday, and S. Hull, Phys. Rev. B **45**, 2613 (1992).

[30] R. G. Greene, H. Luo, and A. Ruoff, Phys. Rev. Lett. **73**, 2075 (1994).

[31] J. M. Léger, J. Haines, and A. Atouf, J. Appl. Crystallogr. **28**, 416 (1995).

[32] L. C. Ming, A. Jayaraman, S. R. Shieh, and Y. H. Kim, Phys. Rev. B **51**, 12 100 (1995).

[33] P. G. Gallardo, Phys. Status Solidi B **182**, K67 (1994).